ELSEVIER

Journal of Chromatography A, 750 (1996) 115–125

JOURNAL OF CHROMATOGRAPHY A

On-line liquid chromatography–electrospray ionization mass spectrometry for determination of the brevetoxin profile in natural "red tide" algae blooms

Yousheng Hua[a], Wenzhe Lu[a], Michael S. Henry[b], Richard H. Pierce[b], Richard B. Cole[a,*]

[a]*Department of Chemistry, University of New Orleans, Lakefront, New Orleans, Louisiana 70148, USA*

[b]*Mote Marine Laboratory, 1600 Thompson Parkway, Sarasota, Florida 34236, USA*

Abstract

Reversed-phase liquid chromatography–electrospray ionization mass spectrometry (LC–ESI-MS) was employed to analyze brevetoxin compounds associated with naturally occurring red tide blooms collected from Sarasota Bay, FL, USA. The LC–ESI-MS method utilizes a C_{18} microbore column with a mobile phase consisting of methanol–water (85:15, v/v), a flow-rate of 8 μl/min and a post-column split ratio of 3:1 (UV-absorbance detector–mass spectrometer). Three known brevetoxins Btx-2, Btx-1 and Btx-3 were detected at 60 μg/l, 10 μg/l and 5.7 μg/l levels, respectively, in the natural red tide bloom samples. This distribution differed quantitatively from that found in red tide culture extract samples. Btx-9 was not detected either in natural red tide bloom extracts or in red tide culture extracts, possibly due to the instability of this compound. An unknown component with a molecular mass of 941 found in the natural bloom extract was postulated to have the structure of a reduced form (hydrogenation of two double bonds in the alkyl side chain) of Btx-5.

Keywords: *Gymnodinium breve*; Brevetoxins; Toxins; Electrospray, mass spectrometry

1. Introduction

"Red tides" are a worldwide natural phenomenon caused by dense growth, or bloom, of dinoflagellates under certain favorable conditions (e.g., water depth, nitrate concentration) in oceans and seas [1,2]. Florida's red tide originates from bloom of the dinoflagellate *Gymnodinium breve*, a toxigenic organism [3], identified by Davis in 1948 [4]. The toxicity of this red tide organism originates from a class of compounds known as brevetoxins, which are characterized by their cyclic polyether structures and their activity in mammals as neurotoxins. Brevetoxins are synthesized and maintained in *G. breve*, a single-celled organism. During episodes of Florida red tide, brevetoxins can be released from the cell of *Gymnodinium breve*. They have caused massive fish kills, respiratory problems (e.g. coughing, sneezing) and eye irritation to humans near the seashore [5–7] and skin irritation to swimmers during red tide outbreaks [8]. In addition to sub-lethal human intoxications, shellfish toxicity was also reported to result from Florida red tide blooms [9]. Shellfish toxicity is believed to be brought on by brevetoxin accumulation during filter feeding [10]. The toxicity mechanism is proposed to be linked to the high brevetoxin binding ability to specific receptor sites on proteins participating in the sodium channel in cellular membranes [11–13]. The consequences of brevetoxin binding include the changing of the membrane

*Corresponding author.

0021-9673/96/$15.00
PII S0021-9673(96)00470-0

potential towards more negative values (depolarizing the membrane, while the normal potential inside the cell wall is between −90 and −40 mV) and the prolongation of the time duration that the sodium channel remains activated [3,13].

The toxic symptoms brought on by exposure to various brevetoxins are generally the same, but significant differences exist in the activity (i.e. dose-response) of particular brevetoxins. At present, up to nine brevetoxins have been fully elucidated in terms of structure [12,14]. The brevetoxins may be classified into two types depending upon the backbone structure (Fig. 1). Brevetoxins belonging to the same category exhibit similar toxicity, as evaluated by ED_{50} values (the toxin concentration at which 50% specific displacement of tritiated Btx-3 binding to rat brain synaptosomes occurs) [15], but significant differences exist between the two types. Type-1 compounds exhibit higher toxicity than type-2 toxins [15]. As investigations of brevetoxin behavior progress, including studies of chemical stability [16], pharmacology [17], morphology and pathophysiology [18], more information has been established concerning distinctions between the behavior of individual brevetoxins.

The development of techniques for separating and detecting individual brevetoxins and their metabolic products has become increasingly important to obtaining accurate information for toxicity evaluation, as well as for investigating mechanistic aspects related to the mode of action. Current methods for brevetoxin analysis are classified into three categories. There are bioassays, based on the toxic response of selected living organisms [19,20]; immunoassays and pharmacologic activity assays, based on the unique biochemical reactions between biomolecules and brevetoxins [15,21] and lastly, chromatographic analyses which enable separation and detection of brevetoxins contained in a mixture [22,23].

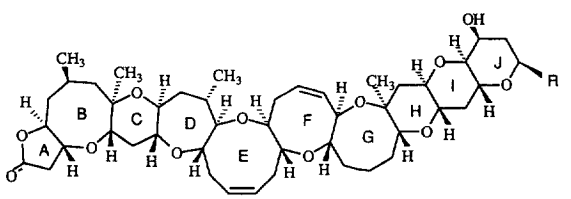

Type-1 Brevetoxins: Btx-1, R = $CH_2C(=CH_2)CHO$
Btx-7, R = $CH_2C(=CH_2)CH_2OH$
Btx-10, R = $CH_2CH(CH_3)CH_2OH$

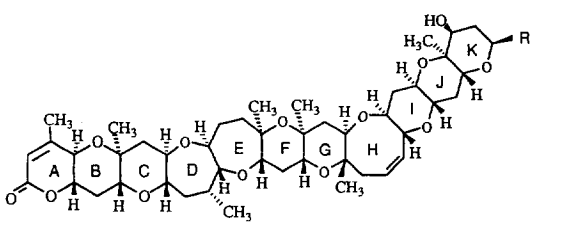

Type-2 Brevetoxins: Btx-2, R = $CH_2C(=CH_2)CHO$
Btx-3, R = $CH_2C(=CH_2)CH_2OH$
Btx-9, R = $CH_2CH(CH_3)CH_2OH$
Btx-5, the K-ring acetate of Btx-2
Btx-6, the H-ring epoxide of Btx-2

Fig. 1. Structures of two classes of brevetoxins.

Among these analytical approaches, only chromatographic methods can provide physical separation and give quantitative information concerning individual brevetoxins contained in a complex sample preparation consisting of several brevetoxins. High-performance liquid chromatography (HPLC) is widely used in brevetoxin purification from different matrices to enable brevetoxin quantitation for analytical and research purposes [22–25]. The UV detector is most commonly used with HPLC systems, including those employed for brevetoxin analysis. However, the UV detector offers relatively low sensitivity compared to other detectors and suffers from interferences from co-eluting chromophores.

Recently, we have developed an on-line HPLC–electrospray ionization mass spectrometry method for brevetoxin analysis in red tide culture extract samples. This developed method features high detection specificity and high sensitivity [26]. In the current report, we expand the applications of LC–ES-MS for brevetoxin analysis to present, for the first time, investigations of the distribution of brevetoxins in naturally occurring red tide blooms found in Sarasota Bay in the Gulf of Mexico, just off the western coast of Florida. In addition, a comparison of LC–UV and LC–ES-MS methods is given for brevetoxin analysis.

2. Experimental

2.1. LC separation conditions

All liquid chromatography separations of brevetoxin were accomplished employing a hydrophobic

3 μm C_{18} microbore column, (Isco, Lincoln, NE, USA), 100×1 mm I.D. with a methanol–water mobile phase. Two precision syringe pumps (Isco, Model 100D) were used to deliver the mobile phase. Samples were injected through a high-pressure, low-dispersion injection valve (Rheodyne 7520, Cotati, CA, USA) that was fitted with a 1.0 μl-sample loop. Experiments to optimize the separation of brevetoxins were conducted using off-line microbore LC–UV, in a manner similar to those described elsewhere [26], employing a CV^4 absorbance detector (Isco) operated at 215 nm. The capacity factors (k') for standard solutions of the brevetoxins Btx-1, Btx-2 and Btx-9 were measured using varied LC mobile phase ratios of methanol–water (90:10, 85:15 and 75:25, v/v) at a flow-rate of 20 μl/min. The k' values measured for the 85:15 ratio were 1.2, 1.4 and 2.2 for Btx-9, Btx-2 and Btx-1, respectively. The 85:15 methanol–water combination was deemed optimal because, compared to the k' values of the other two mobile phase mixtures, these k' values provided adequate separation, yet avoided excessively long analysis times. Flow-rate optimization for the 85:15 ratio was conducted using a 50 ppm Btx-9 solution which was run at flow-rates varied in the range of 2 to 30 μl/min. The optimum flow-rate for LC–UV was determined to be approximately 4 μl/min (minimum plate height, $H=0.024$). For on-line LC–MS work, the higher flow-rate of 8 μl/min was used to shorten the analysis time and to reduce band broadening in the added dead volume (relative to LC–UV) that is inherent to the employed LC–MS system.

2.2. On-line LC–ES-MS

The LC column was simultaneously interfaced to ES-MS and UV detectors via a tee valve (0.1 μl dead volume, Valco, Houston, TX, USA). One outlet of the tee valve was connected to the UV detector via a 20 cm×100 μm I.D. deactivated fused-silica capillary. The other outlet was connected to the electrospray mass spectrometer via the same type of capillary, 32 cm in length. The LC eluent was split post-column in an approximately 3:1 (UV detector–ES-MS detector) ratio.

All mass spectrometry experiments were conducted on a single quadrupole electrospray ionization mass spectrometer (Vestec 201, PerSeptive Biosystems, Houston, TX, USA) with a Vector Two data system (Teknivent, Maryland Heights, MO, USA). During LC–ES-MS operation, LC eluent was introduced into the mass spectrometer ion source through a stainless steel capillary (100 μm I.D., 2 cm length "needle") held at high voltage (+2.6±0.1 kV). The normal "cone-shaped" counter-electrode (also referred to as the "nozzle") was replaced by a flat plate counter-electrode, as described previously [26]. The distance between the needle and the counter-electrode (flat plate) was held constant (15 mm). The voltage at the flat plate and the skimmer-collimator voltage difference were held at 297 and 20 V, respectively. The temperature of the source block was 247±1°C and the temperature in the vicinity of the needle (electrospray chamber) was controlled at 50±1°C (both measured by thermocouple).

2.3. Red tide natural blooms and their extracts

Three replicate natural bloom samples ("sur 1", "sur 2" and "sur 3") were collected from a single site in the Gulf of Mexico. The samples were collected 1/2 mile off shore from New Pass at the south end of Long Boat Key in Sarasota County, FL, during a red tide outbreak on October 26, 1994. The collected bloom samples were treated by osmotic shock to lyse cells and release toxins contained in the cells. The lysed solutions containing brevetoxins were filtered and then extracted by C_{18} solid phase extraction [27] to obtain suitable concentrations for LC–ES-MS determinations. The lysed sur 1, sur 2 and sur 3 bloom samples of 900 ml, 915 ml and 920 ml, respectively, were extracted at a rate of 4 l/h through 4 g C_{18} columns. After extraction, the columns were first eluted with reversed osmosis water to remove any residual salt and were then dried by vacuum aspiration in air. Toxin was eluted from the C_{18} solid phase with a minimum (15 ml) of methanol. The extracts were evaporated to 3 ml and kept refrigerated (−5°C) up until LC–ES-MS analysis.

2.4. Brevetoxin standards

Solutions of the brevetoxin standards Btx-2, Btx-3 and Btx-9 were prepared by individually dissolving 100 μg of the commercially purchased brevetoxins (Chiral, Miami, FL, USA) into 0.2 ml of acetone.

Sample concentrations were adjusted by diluting the above solutions, and standard brevetoxin mixtures, with acetone or methanol–water (85:15, v/v) as the mobile phase. Acetone, methanol and water (all of HPLC grade) were purchased from EM Science (Gibbstown, NJ, USA).

3. Results and discussion

3.1. LC–UV and LC–ES-MS of brevetoxin standards

To evaluate the capability of this on-line LC–ES-MS system for brevetoxin analysis, three known brevetoxin standards, Btx-1, Btx-2 and Btx-9 were analyzed (separately and as a mixture) employing a post-column splitter to permit simultaneous UV and ES-MS detection. Additional unknown peaks were observed in the LC–UV traces of all three brevetoxin standard solutions. All of these extra peaks were not well resolved under the chromatographic conditions used. These unknowns presumably originate from decompositions of brevetoxin compounds which are known to be unstable in protic solvents [16].

The on-line determination of a standard mixture containing 17 ng/μl Btx-9, 20 ng/μl Btx-2 and 20 ng/μl Btx-1 is shown in Figs. 2 and 3. All data shown in these figures correspond to a single HPLC run with post-column splitting to UV and ES-MS detectors. The UV trace showing absorbance (215 nm) vs. time appears in Fig. 2a, while the total ion chromatogram from *m/z* 300–1900 is shown in Fig. 2b. Peak retention times for UV detection were about 1 min shorter than the corresponding ES-MS peaks because of the faster flow-rate and the shorter capillary length to the UV detector. According to the retention times, peaks 4, 5, 7 and 8 correspond to Btx-9, Btx-2, an unknown "U_a" and Btx-1, respectively. The four major peaks in Fig. 2b (labeled 4′, 5′, 7′ and 8′) correspond to these same brevetoxin species which appear in the respective mass spectra chiefly as $[Btx\text{-}9+Na]^+$ (*m/z* 922), $[Btx\text{-}2+Na]^+$ (*m/z* 918), $[U_a+Na]^+$ (*m/z* 922, same value as $[Btx\text{-}9+Na]^+$) and $[Btx\text{-}1+Na]^+$ (*m/z* 890). The designated $[M+Na]^+$ peaks can also contain $[2M+2Na]^{2+}$ species, which have the same *m/z* values as the former. The existence of $[2M+2Na]^{2+}$ species can be postulated due to the observation of $[2M+Na+K]^{2+}$ species reported elsewhere [26]. The

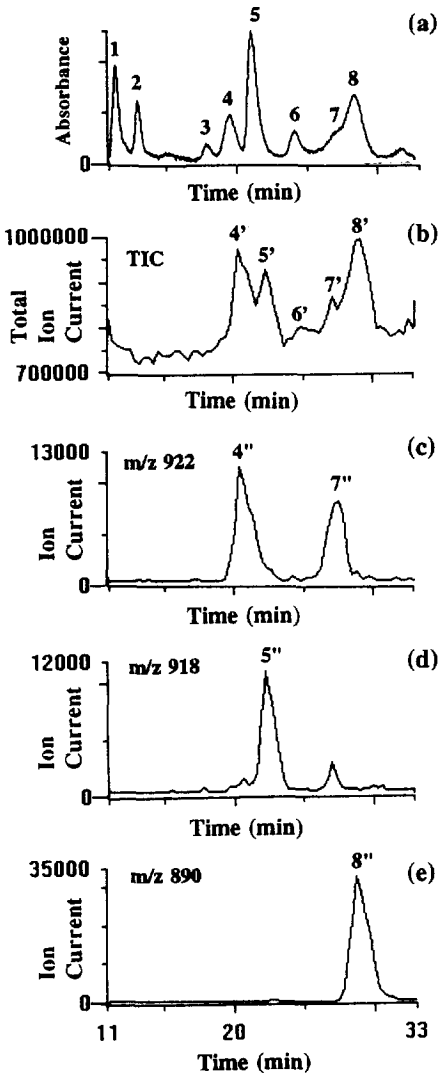

Fig. 2. Simultaneous LC–UV and on-line LC–ES-MS analysis of a mixture of 17 ng/μl Btx-9, 20 ng/μl Btx-2 and 20 ng/μl Btx-1 brevetoxin standards: (a) UV absorbance (215 nm) chromatogram; (b) total ion chromatogram (TIC) *m/z* 300–1900; (c)–(e) reconstructed ion chromatograms of *m/z* 922, *m/z* 918 and *m/z* 890, respectively. The five chromatograms were obtained from a single run. Conditions: 100×1 mm I.D. C_{18} column; methanol–water (85:15, v/v) as the mobile phase at a flow-rate of 8 μl/min; post-column split ratio of 3:1 (UV-absorbance detector–mass spectrometer); injection volume, 1 μl.

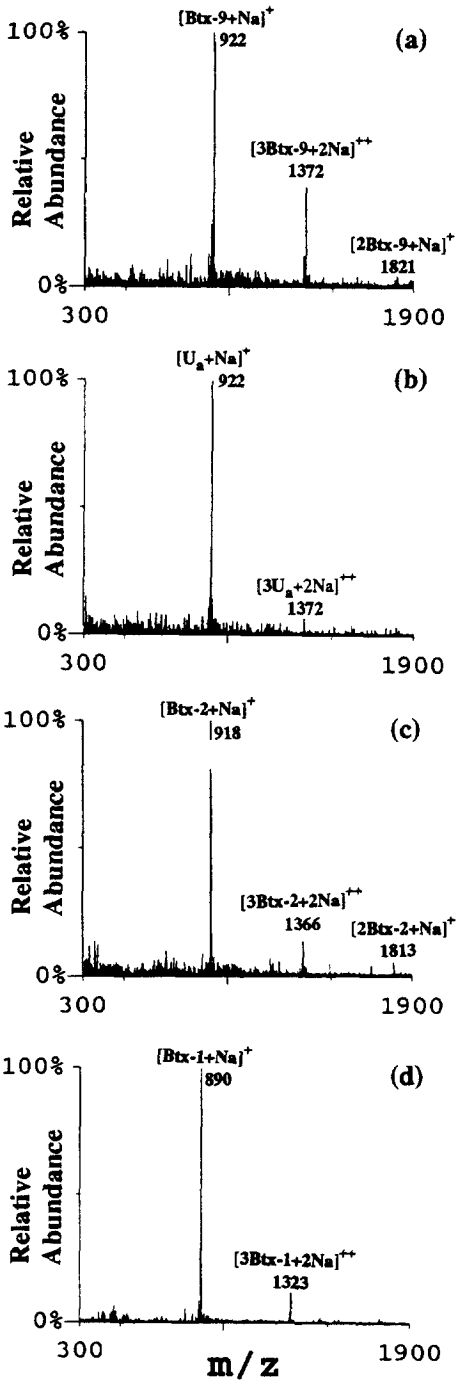

Fig. 3. Electrospray ionization mass spectra obtained as an average of four scans at peak maxima from corresponding selected ion chromatograms: (a) from peak 4″ of Fig. 2c; (b) from peak 7″ of Fig. 2c; (c) from peak 5″ of Fig. 2d; (d) from peak 8″ of Fig. 2e.

impurity peak (6′) in Fig. 2b corresponds to detected ions having m/z values of less than 300. Single ion chromatograms for the above-mentioned m/z 922, 918 and 890 ions are shown in Fig. 2c–e, respectively. ES mass spectra representing the averages of at least four consecutive scans taken from the regions of highest peak intensities (for peaks 4″, 7″, 5″ and 8″ of Fig. 2) are given in Fig. 3a–d, respectively. By comparing the retention times with those obtained from the injections of the individual brevetoxins using LC–UV and on-line LC–ES-MS, and by identifying the characteristic mass spectral pattern of brevetoxins, the chromatographic peaks at 20.1 min (4′, 4″), 22.4 min (5′, 5″) and at 29.1 min (8′, 8″) in Fig. 2 were confirmed to arise from Btx-9, Btx-2 and Btx-1, respectively. The mass spectra taken from the regions of chromatographic peak maxima for each brevetoxin standard (Fig. 3) each exhibit two main ions that correspond to the sodium adduct of the brevetoxin monomer (base peak in each case) and to the doubly charged non-covalently bound trimer (i.e. three brevetoxin molecules solvating two sodium ions). In addition, two small peaks corresponding to singly charged non-covalently bound dimers, i.e., $[2M+Na]^+$, and to protonated brevetoxin molecules, $[M+H]^+$ (appearing at 22 m/z units below the corresponding base peaks) were observed for each chromatographic peak corresponding to the brevetoxin standards. These four brevetoxin related ions are characteristic mass spectral peaks for brevetoxin identification in ES-MS. Direct infusion of these individual brevetoxins into the ES mass spectrometer also produces the same four related ions [26]. Analogs to the ionic trimer and dimer forms observed here were not displayed in ES mass spectra of other ionophoric substances such as okadaic acid and dinophysistoxin-1 [28].

An unknown compound detected as peak (7′, 7″) in Fig. 2b–c appeared at a retention time of 27.0 min; this unknown has been assigned as "U_a". Even though Fig. 2c shows that U_a was well separated from Btx-9 (peak 4″), the mass spectrum of U_a shown in Fig. 3b exhibits two peaks (m/z 922 and 1372) having exactly the same m/z values as the sodium adduct ions of Btx-9 shown in Fig. 2a. This suggests that "U_a" is an isomer of Btx-9, with an average molecular mass of 899. Further LC–ES-MS analysis (not shown) of individual brevetoxin stan-

dards revealed this unknown to be a contaminant of the Btx-1 standard. The unknown U_a and Btx-9 exhibited mass spectral peaks at exactly the same mass values corresponding to the four brevetoxin related ions, but the relative intensities of the four peaks were different. These mass spectral features strongly suggest that U_a, an isomer of Btx-9, belongs to the brevetoxin class of compounds.

The feasibility of quantitating components contained in the brevetoxin mixture was investigated by first examining the possibility of quantitation directly from the LC–UV trace shown in Fig. 2a. From individual injections of three brevetoxins (Btx-1, Btx-2 and Btx-9), it was found that peak 5 (the largest peak in Fig. 2a) did not originate solely from Btx-2. One contaminating component in the Btx-9 solution (low molecular mass giving a mass spectral signal at m/z 198) happens to co-elute with Btx-2 at 22.1 min. Co-eluting components, of course, impair the ability to obtain accurate quantitative results by LC–UV. After calculating the molar absorption coefficient of Btx-2 using a fresh standard solution and after determining the Btx-2 concentration in the sample used to generate Figs. 2 and 3 [from an ES-MS response vs. concentration (calibration) curve], it is estimated that Btx-2 contributes only about half of the area of peak 5 in the UV trace. Additional UV peaks labeled 1, 2, 3 and 6 (Fig. 2a) indicate that the brevetoxin standards may have decomposed and/or contain other impurities that were absent from the solvent blank. These extra components giving UV peaks did not exhibit strong responses in the corresponding ES total ion chromatogram (Fig. 2b) under the employed operating conditions, possibly due to low affinities for sodium ions and protons.

Detection limits of this on-line system for Btx-9, Btx-2 and Btx-1 were determined by injecting brevetoxin mixtures in increasing concentrations, with the mass spectrometer scanning from m/z 859–950 to detect $[M+Na]^+$ forms of the various brevetoxins, while the UV detector monitored absorbance at 215 nm. The detection limits of the UV detector and the ES-MS detector are listed in Table 1. For all three brevetoxins, the ES-MS detector shows lower detection limits, especially for Btx-1, demonstrating ES-MS is highly sensitive for brevetoxin analysis.

Table 1
Detection limits of LC–UV and LC–ES-MS for brevetoxin analysis ($S/N=3$)

	LC–UV (215 nm)	LC–ES-MS
Btx-1	5000 pg	50 pg
Btx-2	3000 pg	1000 pg
Btx-9	6000 pg	600 pg

LC conditions: 100×1 mm I.D. C_{18} column; methanol–water (85:15, v/v) as the mobile phase; injection volume, 1 μl.

3.2. Brevetoxin analysis in natural red tide blooms by on-line LC–ES-MS

The developed on-line LC–ES-MS method with simultaneous UV detection is used here to investigate the distribution of known brevetoxins in natural red tide bloom samples. In addition, this methodology can permit the discovery of other species related to known brevetoxins contained in these samples. Red tide bloom samples were collected off the western coast of Florida near Sarasota Bay during an outbreak in the fall of 1994. As described in Section 2, replicate samples were first subjected to solid phase extraction [27], to clean up the samples (essentially removing highly polar constituents) and to ensure that the concentrations were suitable for LC–UV and LC–ES-MS analyses. The extract samples were simultaneously analyzed by LC–UV (215 nm) and LC–ES-MS with the mass spectrometer scanning from m/z 50–2000. The LC–UV trace for one extract sample (sur 1) is shown in Fig. 4a; the accompanying LC–ES-MS total ion chromatogram (TIC) is shown in Fig. 4b. Reproducibility was tested by repeat injections of the same extract sample. In each case, the intensities of the major peaks differed by less than 10% compared to the first injection. Two replicate extract samples (sur 2 and sur 3) were also analyzed and they showed similar profiles.

Many components are contained in this complex seawater sample. Fig. 4a shows five principal, distinct, peaks and some other weakly responding components. The retention time of peak 5 is close to that of the standard, Btx-2. The TIC (Fig. 4b) plots the sum of all detectable ion signals (total ion current) vs. time. The mass spectrometer, of course, will give a signal for each ionized component that is

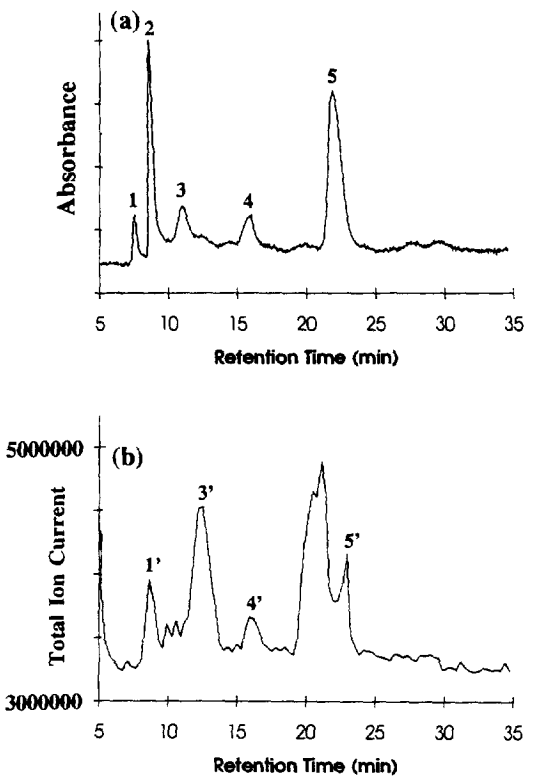

Fig. 4. Simultaneous LC–UV and LC–ES-MS analysis of a natural red tide bloom seawater extract. (a) UV absorbance (215 nm) chromatogram; (b) total ion chromatogram (TIC) m/z 50–1900. The two chromatograms were obtained from a single run. Conditions: 100×1 mm I.D. C_{18} column; methanol–water (85:15, v/v) as the mobile phase at a flow-rate of 8 μl/min; post-column split ratio of 3:1 (UV-absorbance detector–mass spectrometer); injection volume, 1 μl.

transmitted to the detector. The set of components that are present as ionic species in the TIC will intersect the set of absorbing compounds in the UV trace. Careful inspection of the obtained mass spectra over the entire chromatographic time range verifies the truly complex composition of the seawater extract sample. Data reduction consisted of visual inspection of sequentially obtained mass spectra, with particular attention given to the higher mass region (e.g. m/z>800) to identify ions which may represent brevetoxin species. Reconstructed ion chromatograms (Fig. 5) show seven different ions with relatively high abundances and different retention times. Fig. 6 shows the corresponding ES mass spectra representing the average of at least four consecutive scans taken from the region of maximum ion current of the single ion chromatogram displayed in Fig. 5.

By comparing the retention times and ES mass spectral features with those of certain individual brevetoxin standards, several peaks appearing in the ES ion chromatograms could be positively identified. Co-eluting components could be distinguished from each other using mass spectral information, i.e., individual components gave distinct, quantifiable single ion chromatograms when the TIC (and UV) traces did not allow the extraction of such specific information. Even with mass spectral information, differentiation of co-eluting compounds of the same mass (e.g. isomers) can still be a problem.

The distinct peak exhibiting a retention time of 22.2 min corresponding to m/z 918 in Fig. 5d was assigned to the sodium adduct of Btx-2, i.e., $[Btx\text{-}2+Na]^+$. In the corresponding mass spectrum shown in Fig. 6d, four peaks at m/z 896, 918, 1366 and 1813 could be assigned as $[Btx\text{-}2+H]^+$, $[Btx\text{-}2+Na]^+$, $[3Btx\text{-}2+2Na]^{2+}$ and $[2Btx\text{-}2+Na]^+$, respectively. It was found that the reconstructed ion chromatograms of these four ions exhibited elution profiles which overlapped that of the Btx-2 standard, confirming that they originated from Btx-2. Comparing the intensity of m/z 918 to a calibration curve obtained from standard Btx-2, the concentration of Btx-2 in this red tide bloom extract sample was determined to be 18 ng/μl. The concentration of Btx-2 in the natural red tide bloom was calculated as 60 μg/l. In units of micrograms per million *G. breve* cells (μg/MC), the concentration is 12.7 μg/MC. From the LC–UV trace alone (Fig. 4a), the concentration of Btx-2 (peak 5) is estimated to be about 65 ng/μl, using a molar absorption coefficient for Btx-2 determined using pure standard solutions. This higher estimated concentration (compared to 18 ng/μl by ES-MS) may be largely attributable to UV absorption of co-eluting components which interfere with Btx-2 analysis by the LC–UV method. Co-eluting components of m/z 321 and 487 appeared in the mass spectrum obtained in the region of elution of Btx-2 (Fig. 6d). The reconstructed ion chromatograms of these two ions exhibited elution profiles which partially overlapped that of Btx-2. Another co-elut-

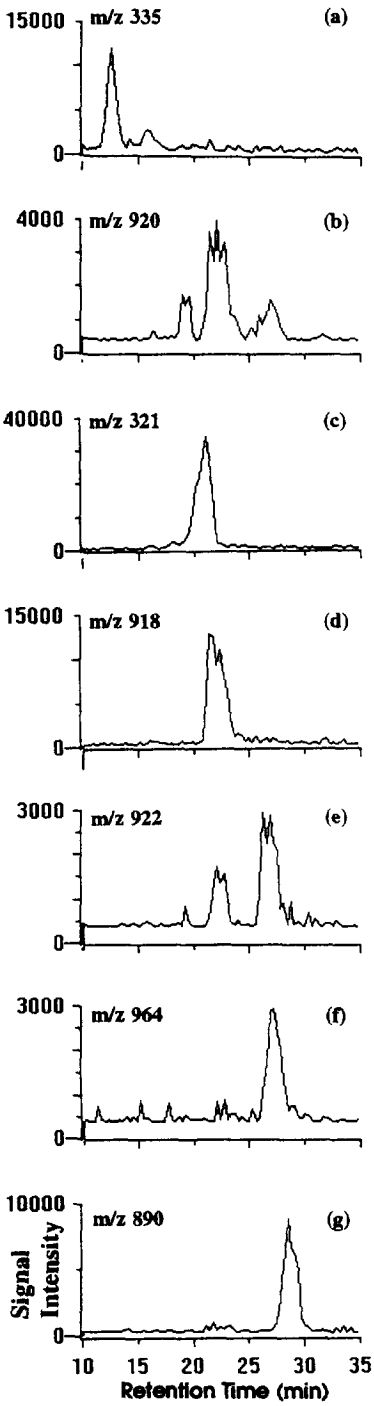

Fig. 5. Reconstructed ion chromatograms for on-line LC–ES-MS analysis of the natural red tide bloom seawater extract.

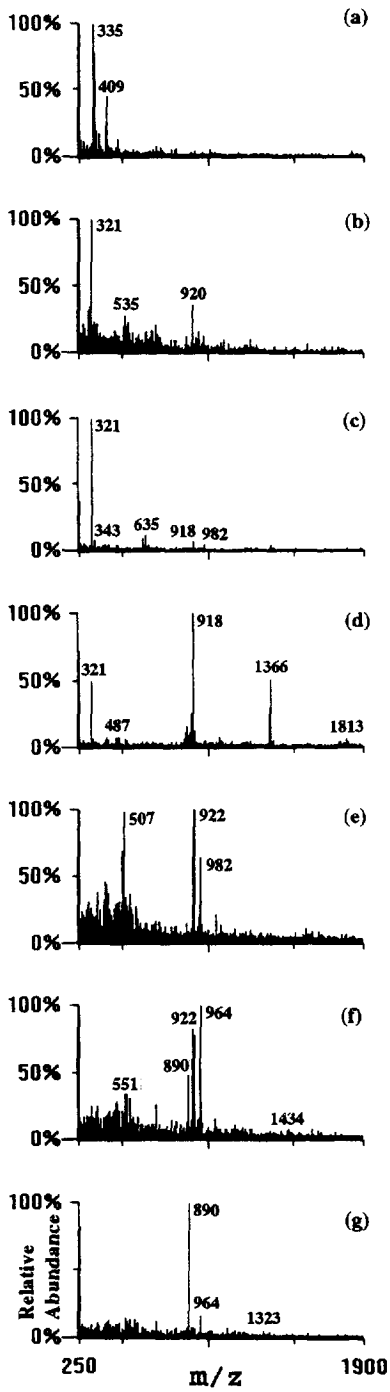

Fig. 6. Electrospray ionization mass spectra obtained as an average of four scans at peak maxima from corresponding selected ion chromatograms (Fig. 5) found immediately to the left of each spectrum, except for (b) which represents an average of four scans at peak maximum from the first peak (19.2 min) in Fig. 5b.

ing component was also observed at m/z 198 (not shown in Fig. 6d) and its reconstructed ion chromatogram also exhibited an elution profile that partially overlapped that of Btx-2. This m/z 198 ion was previously observed in the ES mass spectrum of a partially decomposed Btx-9 standard (left standing for 5 h in the mobile phase solution).

The last eluting peak (Fig. 5g) appeared at 29.0 min, which corresponds to the retention time of Btx-1. The m/z 890 and 1323 peaks correspond to $[Btx\text{-}1+Na]^+$ and $[3Btx\text{-}1+2Na]^{2+}$, respectively. A peak corresponding to $[2Btx\text{-}1+Na]^+$ was not observed at this low concentration. It was previously demonstrated that non-covalently bound trimeric and dimeric forms of three tested brevetoxins decreased in abundance with dilution more rapidly than $[M+Na]^+$ [26]. The concentration of Btx-1 was determined to be 3.0 ng/μl by consultation with a standard Btx-1 calibration curve. This corresponds to a Btx-1 concentration in the natural red tide bloom of 10 μg/l. In units of micrograms per million *G. breve* cells, the concentration is 2.1 μg/MC. In Fig. 5g, the signal-to-noise ratio based upon the peak–peak noise level for the Btx-1 peak is about 45. The LC–UV trace (Fig. 4a), however, reveals a barely detectable peak ($S/N \approx 2$) between 28.5 and 30.3 min, corresponding to the elution time of Btx-1.

There are three peaks in the reconstructed ion chromatogram of m/z 920 (Fig. 5b). The retention time of the first peak (19.2 min) corresponds to that of standard Btx-3, so this peak has been assigned as the sodium adduct of Btx-3, i.e, $[Btx\text{-}3+Na]^+$. From the ES mass spectrum (Fig. 6b) taken from the region of this first peak, m/z 920 appears as a distinct peak, yet the other Btx-3 related ions (doubly charged non-covalently bound trimer and singly charged non-covalently bound dimer) were not observed, possibly due to the low concentration of Btx-3 in the extract sample. The concentration of Btx-3 was estimated (using a Btx-9 calibration curve because Btx-3 and Btx-9 have similar signal responses) to be 1.7 ng/μl in the red tide extract, 5.7 μg/l in the red tide bloom sample and 1.2 μg/MC in units of micrograms per million *G. breve* cells. According to retention times, the other two signals at m/z 920 in Fig. 5b originate from a combination of ^{13}C isotope contributions from other ionic species (e.g. m/z 918) and the low resolution of the quadrupole mass analyzer used ($m/\Delta m \sim 300$). This low resolution implies that the m/z 922 ion can contribute a small signal at m/z 920.

The distinct peak exhibiting a retention time of 27 min, corresponding to m/z 922 in Fig. 5e, was assigned to the sodium adduct of the unknown, U_a, proposed to be an isomer of Btx-9, which was found as a contaminating component in the Btx-1 standard solution (see Fig. 2c). The earlier peak with a retention time of 22.2 min originates from ^{13}C isotopes of m/z 918, which appear due to the low mass resolution.

The most abundant ion, exhibiting a retention time of 21 min, corresponds to m/z 321 in Fig. 5c. The retention time of this unknown peak is very close to that of Btx-2, posing an interference for non-specific (e.g. UV) detection of Btx-2, as previously mentioned. The corresponding mass spectrum of this unknown (Fig. 6c) exhibits ions at m/z 321, 343, 619, 635 and 982. The ion of m/z 321 is proposed to be a protonated form of the unknown, U_e, i.e., $[U_e+H]^+$, and m/z 343 as $[U_e+Na]^+$. Unlike brevetoxin compounds, the trimeric or dimeric ion forms, which invariably appear when the monomer is present in high abundance, were not observed in the mass spectrum of U_e, indicating that this unknown has different mass spectral behavior than the brevetoxin compounds. Other ions at m/z 619, 635 and 982 may originate from other co-eluting unknown components. The ion of m/z 982 was previously observed in a red tide culture extract sample in the same retention time region [26].

An unknown compound, U_f, exhibiting a clear peak with a retention time of 27.2 min, is shown in the reconstructed ion chromatogram of m/z 964 (Fig. 5f). Ions at m/z 964 and 1434 observed in the corresponding mass spectrum (Fig. 6f) were found to have overlapping reconstructed ion chromatograms, suggesting that they originate from the same neutral molecule, U_f, having a molecular mass of 941. The m/z 964 ion was assigned as $[U_f+Na]^+$, and m/z 1434 was assigned as $[3U_f+2Na]^{2+}$. The unknown, U_f, is postulated to belong to the brevetoxin class of molecules, as it expressed mass spectral features similar to those of known brevetoxins. The molecular mass of the neutral molecule (941) is four units higher than that of Btx-5. The structure of U_f could be similar to Btx-5 with hydrogenation (reduction) of

two double bonds in the alkyl side chain, which is analogous to the transformation from Btx-2 to Btx-9. Other peaks shown in Fig. 6f, such as m/z 890 and 922, are likely to originate from the partially co-eluting components Btx-1 and U_a, respectively, considering their close retention times.

Lastly, the reconstructed ion chromatogram of m/z 335 (Fig. 5a) exhibits a retention time of 12.5 min, and a corresponding peak (peak 3, 10.5 min) also existed in the LC–UV trace (Fig. 4a). The ES mass spectrum taken from this region (Fig. 6a) reveals several other co-eluting components, such as m/z 409 and 149 (not shown). These co-eluting species could contribute to the absorption observed in this region of the LC–UV trace (Fig. 4a).

4. Conclusion

To obtain accurate quantitative results describing the brevetoxin profile present in red tide algae blooms, short analysis times are desired. Using C_{18} columns, different brevetoxins can be adequately separated in a methanol–water (85:15, v/v) mobile phase within 35 min. In red tide bloom extract samples, three known brevetoxins, Btx-2, Btx-1 and Btx-3, were detected, with Btx-2 exhibiting the highest concentration. This profile is different from previously analyzed red tide culture extract samples where Btx-3 was not present above the detection limit of about 1 ng/μl. Btx-9 was found neither in red tide bloom extracts nor in red tide culture extracts, possibly due to the instability of this compound.

In comparing LC–UV results with LC–ES-MS, components co-eluting with brevetoxins existed in brevetoxin standard mixtures and in red tide extract samples. These co-eluting components substantially impair both qualitative and quantitative brevetoxin analyses by LC–UV. In LC–ES-MS analysis, however, co-eluting interferences can be distinguished from known brevetoxins by mass spectral information including obtained reconstructed ion chromatograms. In addition to this added specificity in detection, LC–ES-MS also gives lower detection limits than LC–UV for all investigated brevetoxins. Furthermore, the ability of LC–ES-MS to uncover unknown compounds that are structurally similar to the known brevetoxins has been demonstrated. An unknown component with a molecular mass of 941 was found in the red tide bloom extract, whose structure was postulated to be a doubly reduced form of Btx-5 wherein two double bonds in the alkyl side chain are hydrogenated. Although on-line HPLC–ES-MS offers excellent detection specificity and quite low detection limits, this method still cannot be directly applied to the analysis of natural red tide samples without an extraction step prior to analysis. The solid-phase extraction employed serves both to clean-up the sample, by eliminating more polar species, and to concentrate the brevetoxins that are present. Brevetoxin concentrations in the natural environment are often in the ppb range. In future work it is planned to use on-line preconcentration steps to enable direct LC–ES-MS analysis of real samples and to further characterize the structures of brevetoxin decomposition products and other marine toxins.

Acknowledgement

Financial support for this research was provided in part by the Louisiana Education Quality Support Fund [Grant (RF/1995-97)-RD-A-44].

References

[1] R. Margalef, M. Estrada and D. Blasco, in D.L. Taylor and H.H. Seliger (Editors), Toxic Dinoflagellate Blooms, Elsevier/North Holland, 1979, pp. 89–94.
[2] R.C. Dugdale, in D.L. Taylor and H.H. Seliger (Editors), Toxic Dinoflagellate Blooms, Elsevier/North Holland, 1979, pp. 257–262.
[3] M.A. Poli, T.J. Mende and D.G. Baden, Molecular Pharmacol., 30 (1986) 129.
[4] C.C. Davis, Bot. Gaz., 109 (1948) 358.
[5] K.A. Steidinger, Prog. Phycol. Res., 2 (1983) 147.
[6] R.H. Pierce, Toxicon, 24 (1986) 955.
[7] R.H. Pierce, M.S. Henry, L.S. Proffitt and P.A. Hasbrouck, P.A. in E. Granéli, B. Sundström, L. Edler and D. Anderson (Editors), Toxic Marine Phytoplankton, Elsevier, New York, 1990, pp. 397–402.
[8] B.W. Kemppainen, M. Mehta, R. Stafford and R.T. Riley, Toxicon, 30 (1992) 931.
[9] W.H. Hemmert, in V.R. Lociero (Editor), 1st International Conference on Toxic Dinoflagellate Blooms, Wakefield, Massachusetts Science Technology Foundation, 1975, pp. 489.

[10] V.L. Trainer and D.G. Baden, Toxicon, 29 (1991) 1387.
[11] E.A. Catterall and M. Gainer, Toxicon, 23 (1985) 497.
[12] D.G. Baden, FASEB J. 3 (1989) 1807.
[13] G. Strichartz and N. Castle, in H. Hall and G. Strichartz, G. (Editors), Marine Toxins, ACS Symposium Series 418, American Chemical Society, Washington, DC, 1990, pp. 1–20.
[14] K.S. Rein, B. Lynn, R.E. Gawley and D.G.J. Baden, Org. Chem., 59 (1994) 2107.
[15] D.G. Baden, T.J. Mende, A.M. Szmant, V.L. Tranier, R.A. Edwards and L.E. Rozell, Toxicon, 26 (1988) 97.
[16] M.A. Poli, C.B. Templeton, J.G. Pace and G.B. Hines, in S. Hall and G. Strichartz (Editors), Marine Toxins, ACS Symposium Series 418, American Chemical Society, Washington, DC, 1990, pp. 176–191.
[17] R.A. Edwards, V.L. Trainer and D.G. Baden, Mol. Brain Res., 14 (1992) 64.
[18] M. Cattet and J.R. Geraci, Toxicon, 31 (1993) 1483.
[19] Official Methods of Analysis (1984), 14th Ed., Association of Official Analytical Chemists, Arlington, VA, Sections 18.086–18.092.
[20] R.L. Manger, L.S. Leja, S.Y. Lee, J.M. Hungerford and M.M. Wekell, Anal. Biochem., 214 (1993) 190.
[21] F.M. Van Dolah, E.L. Finley, B.L. Haynes, G.J. Doucette, P.D.E. Moeller and J.S. Ramsdell, Nat. Toxins, 2 (1994) 189.
[22] M. Alam, N.M. Trieff and J.E. Hudson, J. Pharm. Sci., 64 (1975) 865.
[23] R.H. Pierce, R.C. Brown and J.R. Kucklick, in D.M. Anderson, A.W. White and D.G. Baden (Editors), Toxic Dinoflagellates, Wiley and Sons, New York, 1985, p. 309.
[24] R.H. Pierce, M.S. Henry, L.S. Proffitt and P.A. Hasbrouck, in E. Granéli, B. Sundström, L. Edler and D. Anderson (Editors), Toxic Marine Phytoplankton, Elsevier, New York, 1990, pp. 397–402.
[25] Y.Y. Lin, M. Risk, S.M. Ray, D. Van Engen, J. Clardy, J. Golik, J.C. James and K.J. Nakanishi, Am. Chem. Soc., 103 (1981) 6773.
[26] Y. Hua, W. Lu, M.S. Henry, R.H. Pierce and R.B. Cole, Anal. Chem., 67 (1995) 1815.
[27] R.H. Pierce, M.S. Henry, L.S. Proffitt and A.J. deRosset, Bull. Environ. Contam. Toxicol., 49 (1992) 479.
[28] S. Pleasance, M.A. Quilliam, A.S.W. de Freitas, J.C. Marr and A.D. Cembella, Rapid Commun. Mass Spectrom., 4 (1990) 206.